



**HAL**  
open science

## Experimental analysis of the impact of an artificially generated tool wear pattern on the residual stress induced by 15-5PH steel turning

F. Clavier, Frédéric Valiorgue, C. Courbon, Joël Rech, H. Pascal, A. Van Robaeys, Y. Chen, J. Kolmacka, H. Karaouni

### ► To cite this version:

F. Clavier, Frédéric Valiorgue, C. Courbon, Joël Rech, H. Pascal, et al.. Experimental analysis of the impact of an artificially generated tool wear pattern on the residual stress induced by 15-5PH steel turning. 6th CIRP Conference on Surface Integrity, CSI 2022, Jun 2022, Lyon, France. pp.394-399, 10.1016/j.procir.2022.04.075 . hal-04092860

**HAL Id: hal-04092860**

**<https://hal.science/hal-04092860>**

Submitted on 22 Jul 2024

**HAL** is a multi-disciplinary open access archive for the deposit and dissemination of scientific research documents, whether they are published or not. The documents may come from teaching and research institutions in France or abroad, or from public or private research centers.

L'archive ouverte pluridisciplinaire **HAL**, est destinée au dépôt et à la diffusion de documents scientifiques de niveau recherche, publiés ou non, émanant des établissements d'enseignement et de recherche français ou étrangers, des laboratoires publics ou privés.



Distributed under a Creative Commons Attribution - NonCommercial 4.0 International License



6<sup>th</sup> CIRP Conference on Surface Integrity (CSI 2022)

## Experimental analysis of the impact of an artificially generated tool wear pattern on the residual stress induced by 15-5PH steel turning

F.Clavier<sup>a\*</sup>, F.Valiorgue<sup>a</sup>, C.Courbon<sup>a</sup>, J.Rech<sup>a</sup>, H.Pascal<sup>a</sup>, A.Van Robaeya<sup>b</sup>, Y.Chen<sup>c</sup>, J.Kolmacka<sup>d</sup>, H.Karaouni<sup>e</sup>

<sup>a</sup> University of Lyon, Ecole Centrale de Lyon - ENISE, LTDS CNRS UMR 5513, 58 Rue Jean Parot, 42000 Saint-Etienne, France

<sup>b</sup> Airbus Helicopters, Aéroport Marseille Provence, 13725 Marignane, France

<sup>c</sup> CETIM, 52, avenue Félix-Louat, 60300 Senlis, France

<sup>d</sup> Framatome Centre Technique, B.P. 40 001 – Saint Marcel, 71328 Chalon sur Saône, France

<sup>e</sup> SAFRAN Tech, Rue des Jeunes-Bois, 78772 Magny-les-Hameaux, France

\* Corresponding author. Tel.: +33 4 77 43 84 00. E-mail address: [florent.clavier@enise.fr](mailto:florent.clavier@enise.fr)

### Abstract

Finish turning is one of the key operations governing the residual stress of functional surfaces. The residual stress state is determined by the cutting conditions and the selected cutting tool system (macro geometry, cutting edge preparation, tool substrate, multi-layer coating...). However, this initial configuration evolves over time due to tool wear. Therefore, it seems very instructive to reproduce the wear process of the tool in order to understand the evolution of thermo-mechanical loadings applied to the machined surface. Flank wear is a parameter which can be difficult to fully control, and it is complex to reproduce experimentally. In this work, a simple, controlled and repeatable method of producing a known flank wear state is introduced and the impact of the flank wear on the surface integrity is assessed. This involves two parts, first reproducing a given flank wear state and second, evaluating experimentally the residual stress induced by the flank wear state on the workpiece. Carbide tools are used to turn 15-5PH steel under dry conditions. It is shown that the method produces consistent results. The effect of flank wear on residual stress is most notable and can generate data to validate numerical modelling. Areas for improving the method are also discussed.

*Keywords:* Tool wear; surface integrity; turning; experimental; residual stresses

### 1. Introduction

The aircraft industry is extremely focused on the fatigue resistance of safety components. During their manufacture, machining processes affect the residual stress state in the vicinity of the functional surface, which is known to play a major role in the fatigue resistance of the machined component [1–5].

In the past, many studies showed that residual stress is greatly affected by the different parameters of the tool/material pair such as the tool geometry [6,7] coating [8], cutting conditions [7,9,10] and material [9,11]. Tool wear also has a great impact on the residual stress gradient at the surface of a machined component. Several research works have already shown the impact of tool wear on residual stress and that its effects can be completely different depending on the tool, workpiece and cutting conditions. Prior studies [11,12]

have highlighted that tool wear drastically shifts the residual stress gradient to a more compressive state with a greater affected depth and higher maximum compressive residual stress. On the contrary, Chen et al. [13] observed a shift of the extreme surface residual stress to higher tensile residual stress values with a similar affected depth. The same evolution of the extreme surface residual stress was observed by Tonshoff et al. [14]. However, a greater affected depth was observed, with higher compressive values and maximal compressive stress.

The differences reported in the literature could either be due to a different interaction with the work material or different wear modes on the cutting tool and thus a different worn geometry. A substantial amount of work remains to be done to understand the effect of tool wear on surface integrity.

Numerical simulation can be seen as a relevant tool to answer this question, and modelling the residual stress induced by a worn tool is still a key issue for the industry.

However, as the wear evolution of a tool can be extremely complex to control in the experiments, it is even more difficult when it comes to a numerical simulation. Understanding how wear affects surface integrity can only be done by simulating initially controlled worn configurations. One solution could be to reproduce the wear process by creating an artificial tool wear that could be better controlled than wear phenomena resulting from a cutting test.

This paper proposes a method to create reproducible artificial worn tools and then investigates the evolution of the residual stress under different levels of controlled tool wear.

## 2. Geometrical model of the tool wear

A previous study has already shown the impact of multiple types of tool wear on the thermo-mechanical loadings and the induced residual stress [15]. It concluded that the flank wear had a major influence on residual stress generation, compared to the wear on the rake face or the modification of the cutting edge radius. The authors thus decided to focus the present work only on the flank wear. The main objective was to create tool wear that could be easily reproduced, and implemented in a numerical simulation. Indeed, most of the time, the flank wear can be very irregular all along the primary and secondary cutting edges. Figure 1a) shows an experimentally worn tool on which the flank wear length can change greatly depending on the considered location. A wear profile was extracted at a given point of the cutting edge and is shown in Figure 1b). Modelling such a complex worn geometry, even in a 2D simulation can be challenging and can lead to severe mesh distortions or local numerical artefacts.

Figure 1 and all the wear measurements were obtained with an ALICONA focus-variation microscope used to build a 3D model of the worn tool (Figure 1a)) and extract the different geometrical features such as the flank wear length, wear angle or cutting edge radius (Figure 1b)).

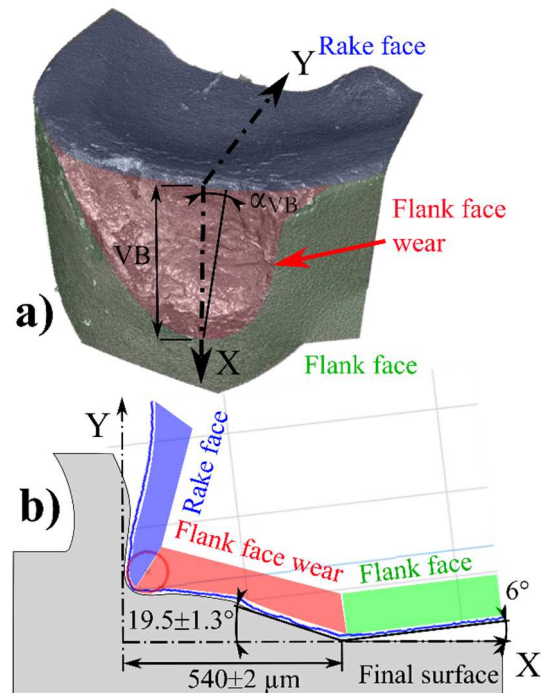


Figure 1 : Worn profile extracted from an experimental cutting tool with a high wear level

From a geometrical perspective, flank wear can be simply represented by a flat surface VB corresponding to the increasing contact length, as well as by a slight inclination angle  $\alpha_{VB}$  (Figure 2b)). The presence of this angle has already been observed in different works [16–19]

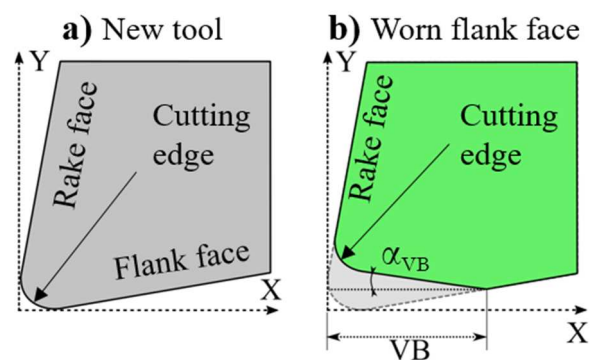


Figure 2 : 2D representation of a new and a worn tool

In order to create artificial worn tools, an NC grinding machine was employed to generate an initial worn geometry (Figure 3). The tool path and grinding wheel orientation were carefully programmed to create different flank wear levels as in the example shown in Figure 3(d). The flank wear angle was the most difficult parameter to control but was found to be in an acceptable and targeted range of 16 to 17°.

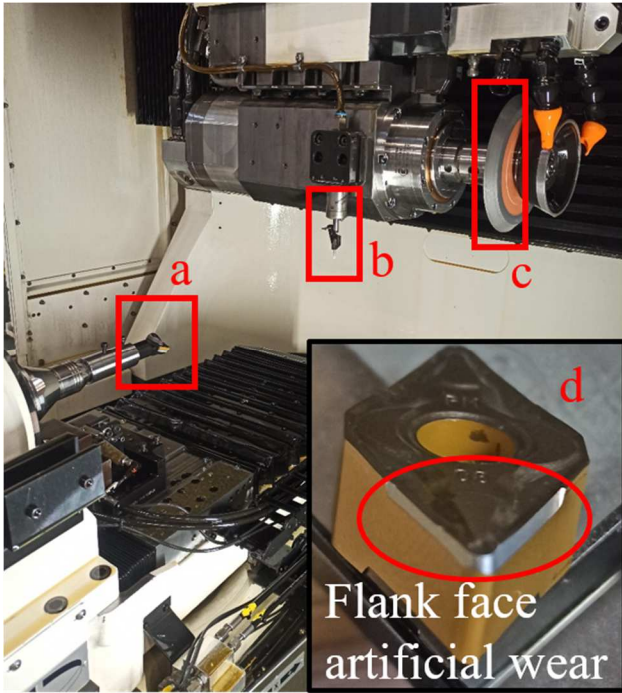


Figure 3 : Grinding machine, tool support (a), contact sensor (b), abrasive wheel (c) are used to create a simplified flank wear (d)

This process was applied to generate 6 artificially worn tools covering 3 different wear states. Figure 4 shows the different generated flank wear VB lengths and  $\alpha_{VB}$  angles for each tool.

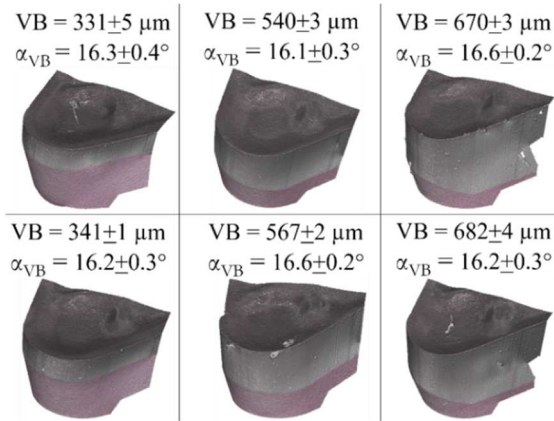


Figure 4 : VB wear levels generated by grinding

In all six cases, the flank wear angle ( $\alpha_{VB}$ ) was about  $16^\circ$ . This angle could be considered as large compared to the values reported in other research works such as [16] or [20] where an angle of  $3^\circ$  was measured. This angle was mostly observed at a really low wear level generated by a light abrasive process. However, when machining more abrasive materials or with more aggressive types of wear such as breaking of the tool edge, larger angles could be observed. On the experimental results shown in Figure 1 and Figure 5, the flank wear angle is respectively 19 and  $14^\circ$ . Even if the wear

of the tool on Figure 1 can be considered as very high, it's not the case for Figure 5.

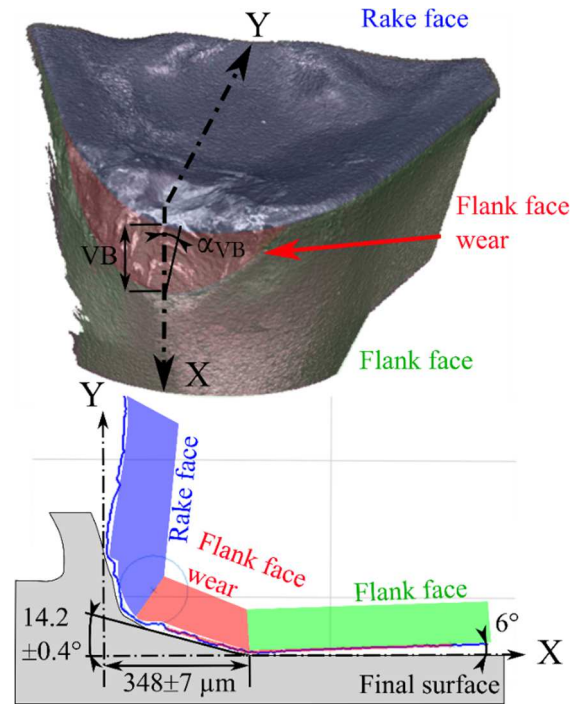


Figure 5 : Worn profile extracted from an experimental cutting tool with a medium wear level

As it can be seen in Figure 6a), the cutting edge radius of the tool after the grinding process is extremely sharp (less than  $10 \mu\text{m}$ ), compared to the cutting edge of the new tool (about  $70 \mu\text{m}$ ). It is also not fully similar to the rounded edge usually observed on a worn tool. In order to avoid any issues such as instabilities or edge breaking during the experiments, the cutting edge was rounded using a Cratex abrasive stick, resulting in a larger and more consistent edge radius as shown in Table 1 and Figure 6b).

Table 1 : Evolution of the cutting edge radius before grinding and after edge preparation

	VB 331 $\mu\text{m}$	VB 540 $\mu\text{m}$	VB 670 $\mu\text{m}$
After grinding	$24 \pm 9 \mu\text{m}$	$19 \pm 5 \mu\text{m}$	$12 \pm 4 \mu\text{m}$
After edge preparation	$74 \pm 7 \mu\text{m}$	$69 \pm 5 \mu\text{m}$	$95 \pm 11 \mu\text{m}$
	VB 341 $\mu\text{m}$	VB 567 $\mu\text{m}$	VB 682 $\mu\text{m}$
After grinding	$19 \pm 7 \mu\text{m}$	$16 \pm 2 \mu\text{m}$	$12 \pm 2 \mu\text{m}$
After edge preparation	$111 \pm 9 \mu\text{m}$	$60 \pm 8 \mu\text{m}$	$74 \pm 2 \mu\text{m}$

This edge preparation was done manually, which explains the difference between one edge and the other. Moreover, this difference can be considered as negligible compared to the amplitude of the investigated flank wear [15].

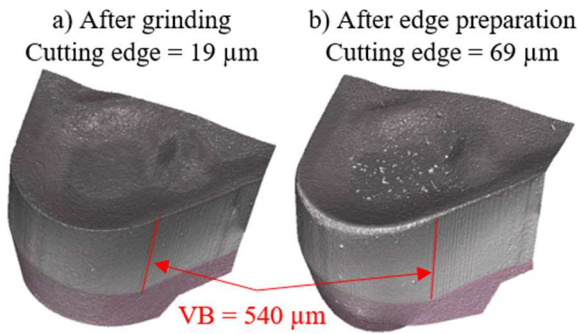


Figure 6 : Cutting edge radius directly after the grinding process a) and once rounded with an abrasive Cratex stick b).

### 3. Experimental campaign with the artificial worn tools

#### 3.1. Cutting condition

Experiments have been performed in order to observe the impact of these 6 artificial worn tools on the residual stress of a machined component. These worn configurations have then been compared to the residual stress induced by a new tool geometry. The cutting insert reference was a DNMG 150608 PM 4325 by Sandvik. The insert is a carbide tool with a CVD Ti (C,N) – Al<sub>2</sub>O<sub>3</sub> coating and was used with the following cutting conditions:  $V_c = 120$  m/min,  $f = 0.2$  mm/rev,  $a_p = 0.2$  mm, dry cutting.

The studied workmaterial was a 15-5 PH stainless steel H1025, which is a martensitic Precipitation-Hardening material with the following mechanical properties: hardness = 35 HRC; tensile strength = 1070 MPa; yield strength = 1000 MPa.

#### 3.2. Measuring set-up

Residual stress was assessed using an X-Ray diffraction method. All the measurements were performed using an iXRD system by PROTO Company, a MG40 head equipped with a 2-mm diameter collimator and following the conditions used in [21].

Electrolytic etching was applied successively at the same location to perform the measurement at different depths.

#### 3.3. Impact on residual stress

For each tool wear state, the two residual stress gradients induced by the two artificially worn inserts are compared to the gradient induced by the new tool geometry and displayed in the following section.

##### Artificial worn tool with a VB around 335 μm

Figure 7 shows that the residual stress profiles generated by the two artificially worn inserts are very similar in both directions (axial and circumferential).

Firstly, this can confirm the stability of the methodology to manufacture artificial tool wear, but also the stability of the machining operation with a tool flank wear. Indeed, machining with this type of geometry could have generated an

unstable process, making the results extremely difficult to analyse.

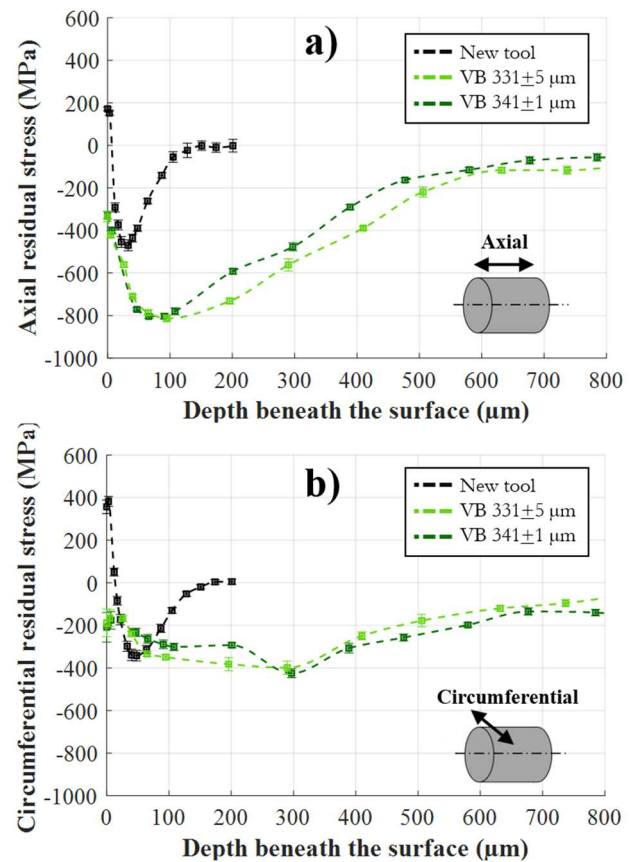


Figure 7 : Comparison between the experimental residual stress gradients of a new tool and the two worn tools with a 331 μm and 341 μm VB

Secondly, the impact of flank wear can be clearly observed in the axial direction with an almost two-time higher maximum compressive stress and a 6-time deeper affected depth compared to the new tool configuration.

In the circumferential direction, the gradient is also greatly impacted by the wear of the tool. The affected depth is also really high, but instead of a single high compressive peak, the maximum stress remains almost constant over the first 300 μm, in a fully compressive state with an almost constant amplitude around -300 MPa.

The extreme surface residual stress is especially modified, shifting from a tensile stress to a compressive one. Indeed, for the new tool, the surface stress was shifted from +200 MPa to -400 MPa for the worn tool in the axial direction and from +400 MPa to -200 MPa for the circumferential direction.

The recorded machining forces for each tool are displayed in Figure 8 and confirm the stability of the process.

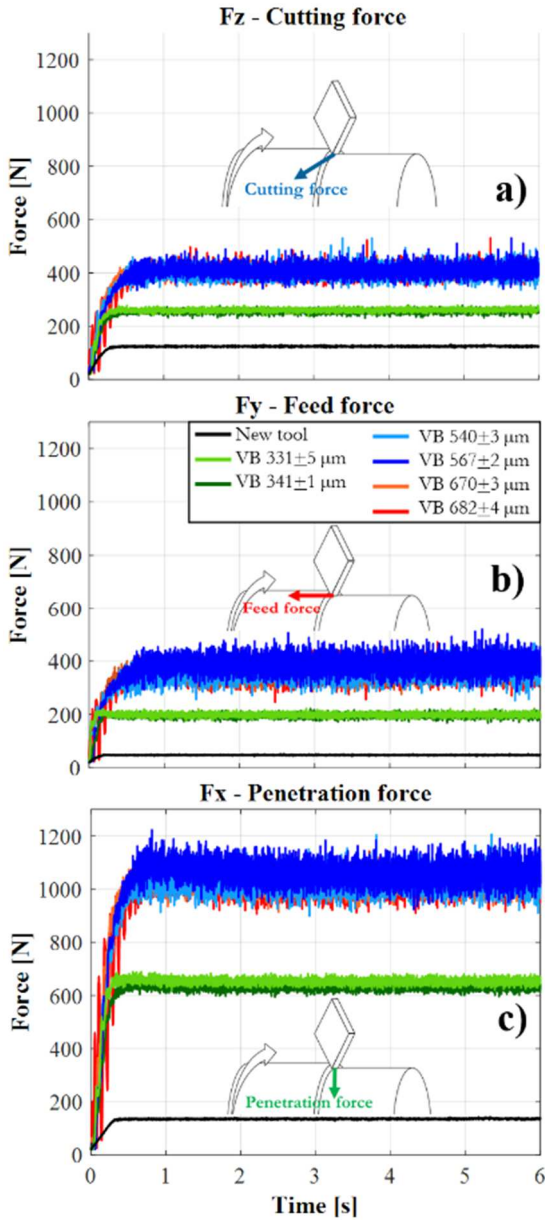


Figure 8 : Comparison between the experimental forces recorded with a new tool and the different artificially worn tools

The greater level of force variation on the worn tools is due to the significant difference in terms of flank contact length compared to the new tool (3 to 7 times higher).

Contact lengths as high as the artificial ones tend to induce a phenomenon of adhesion, with the formation of a stagnation zone under the tool [20]. This creates a cyclic phenomenon which impacts greatly the machining forces: the higher the flank wear length, the higher the variation. Obviously, the forces are greatly impacted by the flank wear, with a significant increase especially regarding the penetration force (Figure 8c)). A similar increase in the cutting forces as well as a change in the residual stress state was also observed in [22].

#### Artificially worn tool with a VB around 550 $\mu\text{m}$ and 700 $\mu\text{m}$

The artificially worn tools with a VB of approximately

550  $\mu\text{m}$  and 700  $\mu\text{m}$  provided similar results in terms of residual stress (Figure 9). This could be due to the already severe wear level generated in both cases, tending to show that a threshold could be reached.

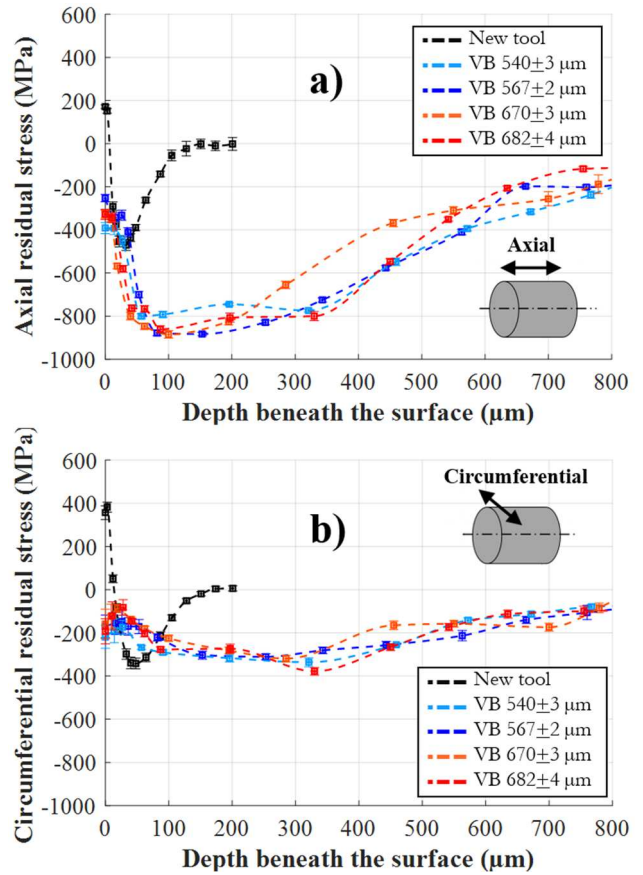


Figure 9 : Comparison between the experimental residual stress gradients of a new tool and the artificially worn tools with a 540  $\mu\text{m}$ , 567  $\mu\text{m}$ , 670  $\mu\text{m}$  and 682  $\mu\text{m}$  VB wear state

The effect of these two VB wear levels is similar to the 331  $\mu\text{m}$  and 341  $\mu\text{m}$  VB configurations, especially in the circumferential direction (Figure 9b)) with the same constant value of -300 MPa.

In the axial direction (Figure 9a)), the maximum compressive stress is slightly higher, around -900 MPa, and affects a deeper region, around 700  $\mu\text{m}$ . The maximum compressive value is also located at a larger depth range: 250  $\mu\text{m}$  for Figure 9a) compared to 50  $\mu\text{m}$  for Figure 7a) and less than 10  $\mu\text{m}$  with the new tool.

The extreme surface residual stress value undergoes exactly the same shift as with the flank wear around 335  $\mu\text{m}$ , confirming that flank wear could even have a beneficial impact.

#### 4. Discussion of results

As seen in the previous section, tool flank wear has a major impact on the residual stress gradient induced on the final machined surface.

In the axial direction, a great increase of the maximum compressive stress was observed, as well as a higher affected

depth, compared to a new tool. Those increases can be directly related to the thermo-mechanical loadings which are much higher with the worn tools than with the new tool. Heat flux generation and normal stress are especially concerned as already observed in a previous work, with a lower flank wear angle [20]. In this study, with a more important flank wear angle, the mechanical impact of the wear must be even higher, resulting in a greater affected depth and higher maximum compressive stress. This drastic increase in the mechanical loadings also shifts the extreme surface residual stress from tensile to compressive values.

In the circumferential direction, the conclusion is really different. Indeed, when using a new tool, no difference in the residual stress gradients between the two directions was observed, whereas major modifications of the stress profiles occurred when using artificially worn tools. This effect is supposed to be the result of an increase in the contact length rather than in the flank wear angle, which generates a longer exposure time to a given heat source. If one considers one material point at the surface and subsurface, the latter will withstand a heat flux 4 times longer with a VB around 335  $\mu\text{m}$ , 7 times longer with a VB around 550  $\mu\text{m}$  and almost 9 times longer with a VB around 700  $\mu\text{m}$ , compared to a new tool. The amount of generated heat is also much lower when machining with a new tool, which can be connected to the change in stress amplitude.

Differences reported in the two directions in terms of residual stress can however be explained by observing the spatial distribution of the heat over a larger area as schematically presented in Figure 10. The material along the circumferential direction, i.e. the cutting direction, is subjected to a much more important thermal gradient than in the axial direction (feed) due to the predominant heat propagation. The specific residual stress gradient observed in the circumferential direction, constant and with a compressive stress around 300 MPa, can also be explained by this analysis.

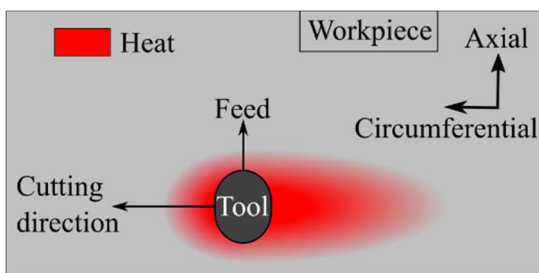


Figure 10 : Schematic of the heat propagation in the cutting and feed direction

## 5. Conclusions

This study first presented a method to generate experimentally an artificially worn tool with a flank wear profile which can be easily replicated and with a great stability through the machining process. It appears as a relevant starting point to study the impact of wear on residual stress gradient and leads to a worn geometry which can be easily implemented in a numerical simulation. 6 cutting tools covering 3 flank wear states were generated with this method. An experimental campaign was then conducted using each of

them to investigate their impact on the residual stress state in finishing turning.

Concerning the residual stress gradients, several conclusions were drawn:

- An increase in the tool flank wear drastically extends the affected depth of residual stress;
- Tool flank wear is able to shift the extreme surface residual stress in a compressive state and to increase greatly the value of the compressive stress peak.
- A threshold can be expected as an increase of VB from 500 to 700  $\mu\text{m}$  will slightly increase the affected depth and the maximum compressive stress, but will mostly change the depth at which this peak is located;
- Compared to the new tool which presents similar residual stress gradients in both directions, worn tools show differences in the circumferential direction with a relatively constant compressive state, around 300 MPa. On the contrary, in the axial direction, the shape was more similar to the profile extracted with a new tool.

The perspective of this work will be to simulate the residual stress corresponding to the 3 wear states presented in this work and compare them with the experimental data.

## Acknowledgments

Authors would like to express their gratitude to AIRBUS HELICOPTERS, FRAMATOME, SAFRAN, CETIM and the ANR for their financial support or contribution within the industrial chair MISU.

## Reference

- [1] Rech, J., Hamdi, H., Valette, S., 2008, Rédaction du chapitre 3 dénommé "Surface finish and integrity", Titre de l'ouvrage édité par J. Paulo Davim: «Machining: fundamentals and recent advances», Springer 2. London: Springer London.
- [2] Smith, S., Melkote, S. N., Lara-Curzio, E., Watkins, T. R., Allard, L., et al., 2007, Effect of surface integrity of hard turned AISI 52100 steel on fatigue performance, *Materials Science and Engineering A*.
- [3] Jawahir, I. S., Brinksmeier, E., M'Saoubi, R., Aspinwall, D. K., Outeiro, J. C., et al., 2011, Surface integrity in material removal processes: Recent advances, *CIRP Annals - Manufacturing Technology*
- [4] Guo, Y. B., Warren, A. W., Hashimoto, F., 2010, The basic relationships between residual stress, white layer, and fatigue life of hard turned and ground surfaces in rolling contact, *CIRP Journal of Manufacturing Science and Technology*
- [5] Yang, X., Liu, C. R., Grandt, A. F., 2002, An experimental study on fatigue life variance, residual stress variance, and their correlation of face-turned and ground Ti 6Al-4V samples, *Journal of Manufacturing Science and Engineering, Transactions of the ASME*, 124/4:809–819
- [6] Hua, J., Umbrello, D., Shivpuri, R., 2006, Investigation of cutting conditions and cutting edge preparations for enhanced compressive subsurface residual stress in the hard turning of bearing steel, *Journal of Materials Processing Technology*, 171/2:180–187
- [7] Dahlman, P., 2004, The influence of rake angle, cutting feed and cutting depth on residual stresses in hard turning, *Journal of Materials Processing Technology*, 147:181–184
- [8] Outeiro, J. C., Pina, J. C., M'Saoubi, R., Pusavec, F., Jawahir, I. S., 2008, Analysis of residual stresses induced by dry turning of difficult-to-machine materials, *CIRP Annals - Manufacturing Technology*
- [9] Caruso, S., Umbrello, D., Outeiro, J. C., Filice, L., Micari, F., 2011, An experimental investigation of residual stresses in hard machining of AISI 52100 steel, *Procedia Engineering*, 19:67–72

- [10] Matsumoto, Y., Hashimoto, F., Lahoti, G., 1999, Surface Integrity Generated by Precision Hard Turning. *Annals of the CIRP* vol.48, p. *Annals of the CIRP* vol.48, 59-62.
- [11] Chandrasekaran, H., M'Saoubi, R., Högman, B., Nordh, L. G., Coulon, B., et al., 2005, Development of machinability enhanced tool steels for improved product economy in hard milling. .
- [12] Liu, M., Takagi, J. I., Tsukuda, A., 2004, Effect of tool nose radius and tool wear on residual stress distribution in hard turning of bearing steel, *Journal of Materials Processing Technology*, 150/3:234–241
- [13] Chen, L., El-Wardany, T. I., Harris, W. C., 2004, Modelling the effects of flank wear land and chip formation on residual stresses, *CIRP Annals - Manufacturing Technology*, 53/1:95–98
- [14] Tonshoff, H. K., Arendt, C., Ben Amor, R., 2000, Cutting of hardened steel, *CIRP Annals - Manufacturing Technology*, 49/2:547–566
- [15] Clavier, F., Valiorgue, F., Courbon, C., Dumas, M., Rech, J., et al., 2020, Impact of cutting tool wear on residual stresses induced during turning of a 15-5 PH stainless steel, *Procedia CIRP*, 87:107–112
- [16] Ducobu, F., Arrazola, P. J., Rivière-Lorphèvre, E., Filippi, E., 2015, Finite element prediction of the tool wear influence in Ti6Al4V machining, in *Procedia CIRP*.
- [17] Lane, B. M., Dow, T. A., Scattergood, R., 2013, Thermo-chemical wear model and worn tool shapes for single-crystal diamond tools cutting steel, *Wear*, 300/1–2:216–224
- [18] Hosseinkhani, K., Ng, E., 2013, Analysis of the cutting mechanics under the influence of worn tool geometry, *Procedia CIRP*, 8:117–122
- [19] Saha, S., Deb, S., Bandyopadhyay, P. P., 2022, Precise measurement of worn-out tool diameter using cutting edge features during progressive wear analysis in micro-milling, *Wear*, 488–489/July 2021:204169
- [20] Clavier, F., Valiorgue, F., Courbon, C., Rech, J., Robaey, A. Van, et al., 2021, Numerical analysis of the tribological and geometrical impacts of tool wear on the thermomechanical loadings induced by 15-5PH steel turning, *Procedia CIRP*, 102:411–416
- [21] Methon, G., Valiorgue, F., Dumas, M., Van-Robaey, A., Masciantonio, U., et al., 2019, Development of a 3D hybrid modeling of residual stresses induced by grooving, *Procedia CIRP*, 82:400–405
- [22] Fernández-Valdivielso, A., López De Lacalle, L. N., Urbikain, G., Rodríguez, A., 2016, Detecting the key geometrical features and grades of carbide inserts for the turning of nickel-based alloys concerning surface integrity, *Proceedings of the Institution of Mechanical Engineers, Part C: Journal of Mechanical Engineering Science*, 230/20:3725–3742